Structural and magnetic properties of double perovskites $AA'FeMoO_6$ ($AA' = Ba_2$, BaSr, Sr_2 and Ca_2)

2000 J. Phys.: Condens. Matter 12 8295

(http://iopscience.iop.org/0953-8984/12/38/306)

J. Phys.: Condens. Matter **12** (2000) 8295–8308. Printed in the UK PII: S0953-8984(00)13693-8

Structural and magnetic properties of double perovskites $AA'FeMoO_6$ ($AA' = Ba_2$, BaSr, Sr_2 and Ca_2)

C Ritter†, M R Ibarra‡, L Morellon‡§, J Blasco‡, J García‡ and J M De Teresa‡

† Institut Laue–Langevin, Boîte Postale 156, 38042 Grenoble Cédex 9, France
‡ Departamento de Física de la Materia Condensada and Instituto de Ciencia de Materiales de Aragón, Universidad de Zaragoza and Consejo Superior de Investigaciones Científicas, 50009 Zaragoza, Spain

E-mail: morellon@posta.unizar.es

Received 3 May 2000, in final form 4 July 2000

Abstract. Room temperature x-ray diffraction, magnetization and neutron diffraction measurements up to 500 K have been carried out on polycrystalline bulk double perovskites $AA'FeMoO_6$ ($AA' = Ba_2$, BaSr, Sr_2, Ca_2) in order to determine and correlate their structural and magnetic properties. As the average ionic radius is diminished, the crystallographic structure evolves from cubic (for $AA' = Ba_2$, BaSr) to tetragonal (Sr_2) and finally to monoclinic (Ca_2). In the case of $AA' = Sr_2$, a novel crossover from a high temperature paramagnetic cubic state to a low temperature ferrimagnetic tetragonal state has been observed. For all the studied compounds, neutron diffraction patterns and magnetization measurements are consistent with a ferrimagnetic ordering of the Fe and Mo sublattices. A remarkable correlation is found between the Curie temperature and the electronic bandwidth, which is controlled by structural parameters.

1. Introduction

Half-metallic compounds, i.e. compounds with only one spin direction present at the Fermi level, are interesting for their potential applications at room temperature in *spin electronics* [1]. Some magnetic oxides have been identified as candidates to exhibit half-metallicity at low temperatures, but the spin polarization is either strongly reduced or negligible at room temperature [2]. In this sense, oxides with both high spin polarization and high Curie temperatures are desirable. Recently, Kobayashi *et al* [3] have reported a high spin polarization for an oxide material with an ordered double-perovskite structure, Sr_2FeMoO_6. Its high Curie temperature, $T_C \approx 420$ K, makes it a promising candidate to work at room temperature. In order to explore other prospective compounds of the same family that could be useful for this purpose, we have investigated the structural and magnetic properties of some $AA'FeMoO_6$ bulk polycrystals (with $AA' = Ba_2$, BaSr, Sr_2, Ca_2). As we summarize in this section, the existing data on the structural, magnetic and conduction properties of these double perovskites are scarce and, definitely, further studies are needed.

In the 1960s, Galasso *et al* [4] studied some compounds of the type $AA'FeMoO_6$ and reported at room temperature a cubic structure for $AA' = Ba_2$, a tetragonal one for $AA' = Sr_2$ and an orthorhombic one for $AA' = Ca_2$, as well as a maximum Curie temperature for

§ Corresponding author: Dr L Morellon, Departamento de Física de la Materia Condensada—ICMA, Facultad de Ciencias, Universidad de Zaragoza—CSIC, Pedro Cerbuna 12, 50009 Zaragoza, Spain.

0953-8984/00/388295+14$30.00

Table 1. Saturation magnetization (M_s) at 5 K and 295 K, Curie temperature (T_C) and room-temperature crystallographic structure as determined from x-ray diffraction of the double perovskites $AA'FeMoO_6$ ($AA' = Ba_2$, BaSr, Sr_2, Ca_2).

Nominal composition	M_s(5 K) (μ_B fu^{-1})	M_s (295 K) (μ_B fu^{-1})	T_C (K)	Cell parameters
Ba_2FeMoO_6	3.53	1.33	308	Cubic $Fm3m$ $a = 8.0697(2)$ Å
$BaSrFeMoO_6$	3.40	1.89	340	Cubic $Fm3m$ $a = 7.9798(2)$ Å
Sr_2FeMoO_6	2.95	1.78	385	Tetragonal $P4_2/m$ $a = 5.5724(2)$ Å $c = 7.9006(2)$ Å
Ca_2FeMoO_6	3.51	2.22	365	Monoclinic $P2_1/n$ $a = 5.4131(2)$ Å $b = 5.5209(2)$ Å $c = 7.7065(2)$ Å $\beta = 89.95(5)^\circ$

$AA' = Sr_2$ ($T_C \approx 420$ K). Similar results were reported by Nakagawa [5], who also claimed that 8% oxygen vacancies hardly modifies the lattice constants and the magnetic behaviour. More recently, Borges *et al* [6] have reported a $P2_1/n$ monoclinic structure for $AA' = Ca_2$ and slightly different Curie temperatures. In this sense, Ogale *et al* [7] have predicted by means of Monte Carlo simulations that Fe/Mo disorder and oxygen vacancies can dramatically lower the Curie temperature. Of special interest is the issue of the intrinsic conduction mechanism existing in these systems, which brings about metallic values of resistance. In these compounds the Fe ions are supposed to be in a high-spin state with all the spin-up 3d orbitals occupied. Sleight and Weiher [8] proposed that if the spin-down 3d orbitals of Fe have similar energy to the 4d orbitals of Mo, they can form a narrow band and provide the conduction mechanism. This is supported by band calculations, which show at the Fermi level a mixing of the spin-down 2p, 3d and 4d bands of O, Fe and Mo respectively [3]. Moreover, this negatively-spin-polarized conduction would be the origin of the extrinsic strong magnetoresistance associated with spin-polarized tunnelling between adjacent grains that has been recently found by different authors in polycrystalline samples [3, 6, 9–11], epitaxial thin films [12, 13] and in artificial grain boundaries [14]. A better understanding of the factors that control the structural, magnetic and conduction properties in these compounds seems crucial in order to optimize their properties for the aforementioned applications.

In this article we address ourselves to study in detail the crystallographic structure of these compounds by using x-ray and high-resolution neutron diffraction, as well as its relationship with the magnetic behaviour. In fact, the Curie temperature seems to be controlled by structural parameters, which influence the electronic bandwidth. The role of the Fe and Mo sublattices on the magnetic structure and conduction mechanisms is also discussed.

2. Experiment

The $AA'FeMoO_6$ ($AA' = Ba_2$, BaSr, Sr_2, Ca_2) samples were prepared by solid state reaction. Stoichiometric amounts of $BaCO_3$, $SrCO_3$, $CaCO_3$, Fe_2O_3, and MoO_3 were mixed, ground and calcined at 900 °C for 2 hours in air. The calcined mixtures were reground, pressed and sintered at 1200 °C for 2 days in a current flow of H_2/Ar (2/98%) with intermediate grindings.

Room-temperature x-ray diffraction patterns were collected using a D-max Rigaku system with rotating anode. This device was operated at 40 kV and 80 mA and a graphite monochromator was used to select the Cu $K\alpha_{1,2}$ radiation.

Magnetization was measured using a commercial (Quantum Design) SQUID magnetometer in fields up to 5 T. T_C was determined by means of a Faraday balance in the range 300–500 K.

Neutron diffraction experiments were carried out on the high resolution powder diffractometer D2B ($\lambda = 1.6$ Å) and the high intensity powder diffractometer D1B ($\lambda = 2.52$ Å), both at the ILL, Grenoble. For all measured compounds, the exact stoichiometry and possible cation disorder was determined using D2B data obtained above the respective Curie temperatures. Sr_2FeMoO_6 was measured at several temperatures on D2B: 2 K, 100 K, 200 K and between 300 K and 500 K in steps of 10 K. The data were analysed using the Rietveld refinement program FULLPROF [15].

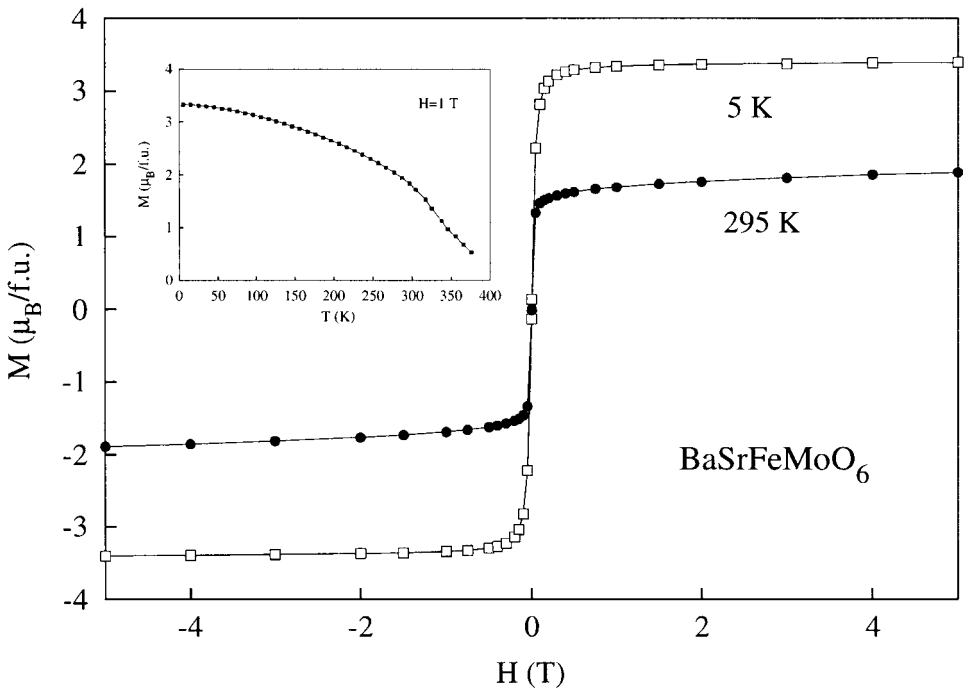

Figure 1. Magnetization isotherms of $BaSrFeMoO_6$ at 5 K (□) and 295 K (●). The thermal dependence of the magnetization in an applied magnetic field of 1 T is shown in the inset.

3. Results from x-ray and magnetization measurements

The quality of the samples and their crystallographic structure has been investigated by means of room-temperature x-ray diffraction. The Rietveld profile analysis of the spectra (FULLPROF [15]) revealed that all compounds are essentially single phase with the exception of Sr_2FeMoO_6, that showed two minor impurity phases (2% of Sr_2MoO_6 and 0.5% of $SrMoO_4$). The cell parameters obtained and the space group used in the refinements are reported in table 1. The values for the cubic compounds ($AA' = Ba_2$, BaSr) are in very good agreement with those reported by Galasso *et al* [4]. Sr_2FeMoO_6 has been fitted in the tetragonal $P4_2/m$ symmetry, yielding values of the cell parameters in close agreement with those reported in [3, 16]. No significant difference in the fit is found either by using the $P4_2/m$ or the $I4/mmm$ space group. The choice of $P4_2/m$ will be justified in section 4.3. Ca_2FeMoO_6 is found to be monoclinic ($P2_1/n$) as previously reported by Borges *et al* [6]. Considering a perfect ordering of the two transition metal sublattices and the nominal stoichiometry, we obtained reliability factors,

R_{Bragg}, ranging between 3.8 and 5.4% for all samples. Different structural models considering either a disorder between Fe and Mo atomic positions or an off-stoichiometric composition, did not improve significantly the fits.

The magnetization isotherms are typically ferromagnetic with negligible remanence and coercivity as illustrated in figure 1 for $BaSrFeMoO_6$. The saturation magnetization at 5 K for all the studied compounds is listed in table 1. In all cases the obtained values are consistent with a ferrimagnetic state but below the expected 4 μ_B fu^{-1} for a nominal ionic configuration $Fe^{3+}(S = 5/2)/Mo^{5+}(S = 1/2)$. This discrepancy could be attributed to the effect of mis-site disorder on the octahedral cation sublattices (Fe, Mo) and/or the presence of oxygen vacancies [7]. Nevertheless, other effects such as covalent mixing with the unpolarized 2p(O) orbitals cannot be ruled out. The high value of the magnetization at 295 K (≈60%) could lead to a high spin polarization at room temperature, with the only exception of Ba_2FeMoO_6 that shows a slightly smaller value ≈38%, as expected from the smaller value of the Curie temperature. The T_C values are slightly lower than those reported in [4] ($T_C = 334, 422, 377$ K for $AA' = Ba_2$, Sr_2, Ca_2) but higher than the ones reported in [6] except for Ba_2FeMoO_6 ($T_C = 367, 371, 345$ K for $AA' = Ba_2$, Sr_2, Ca_2). As already commented, the exact stoichiometry, cation mis-site disorder and oxygen vacancies may have a strong impact on the exact values of both saturation magnetization and Curie temperature. Since we could not evaluate the relative importance of those effects from our x-ray results, a detailed study of both crystallographic and magnetic structure has been performed by means of high resolution powder neutron diffraction.

Table 2. Refined structural and magnetic parameters from neutron powder-diffraction data for the Ba_2FeMoO_6 and $BaSrFeMoO_6$ compounds at 2 K (D1B) and 500 K (D2B).

	$Ba_2Fe_{0.92(1)}Mo_{0.93(1)}O_{5.69(4)}$		$BaSrFe_{0.95(1)}Mo_{0.97(1)}O_{5.84(3)}$	
	2 K	500 K	2 K	500 K
a (Å)	8.0121(5)	8.112 54(7)	7.9272(4)	8.01684(7)
x_{O1}	0.2556(8)	0.2580(4)	0.2532(9)	0.2549(3)
Mo–O1 (Å)	1.958(7)	1.963(3)	1.956(8)	1.965(3)
Fe–O1 (Å)	2.048(7)	2.093(3)	2.008(8)	2.044(3)
$\langle d$(Fe(Mo)–O)$\rangle$	2.003	2.028	1.982	2.005
μ_{Fe} (μ_B)	4.06(9)	—	4.32(8)	—
μ_{Mo} (μ_B)	−0.1(1)	—	0.06(10)	—
R_{Bragg}	3.3	3.4	2.2	3.6
R_{Magn}	4.2		2.4	
χ^2		3.0		2.6

4. Results from neutron diffraction experiments

In a first step, we proceeded to refine the exact stoichiometry for all samples from high resolution spectra at 500 K, i.e. above the Curie temperature. We have included data on a second Sr_2FeMoO_6 (II) sample, which had already been measured and reported in a previous publication [9]. All compounds are cubic ($Fm3m$) at this temperature except for Ca_2FeMoO_6 that adopts the well known $P2_1/n$ structure in double perovskites. The results are as follows: $Ba_2Fe_{0.92}Mo_{0.93}O_{5.7}$, $BaSrFe_{0.95}M_{0.97}O_{5.84}$, $Ca_2(Fe_{0.94}Mo_{0.06})MoO_6$, $Sr_2Fe_{0.97}Mo_{0.99}O_{5.96}$ (I) and $Sr_2Fe_{0.97}Mo_{0.94}O_{5.81}$ (II). No cation disorder was detected for the cubic compounds. In Ca_2FeMoO_6, about 6% of Mo is present on Fe sites, but no Fe on Mo sites could be refined. Comparing the two Sr_2FeMoO_6 samples, one sees that they differ slightly in stoichiometry, the new sample (I) being very close to the ideal composition. All

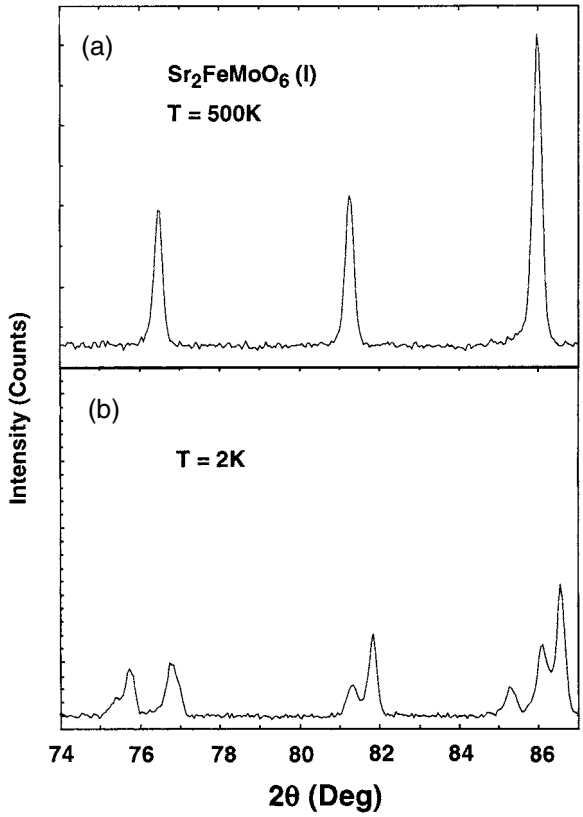

Figure 2. Detail of the angular range $2\theta = 74$–87° of the neutron diffraction pattern of Sr_2FeMoO_6 (I, this work) at 500 K (a) and at 2 K (b) as recorded on the high-resolution instrument D2B.

cubic compounds are slightly oxygen deficient, while the Ca compound has a perfect 2–1–1–6 composition: $Ca_2(Fe_{0.94}Mo_{0.06})MoO_6$. Due to the different behaviour of the compounds we will present the results obtained separately in the remainder of the paper.

4.1. Ba_2FeMoO_6, $BaSrFeMoO_6$

Both compounds stay cubic down to 2 K; the structural parameters are shown in table 2. The O_6-octahedron around the Fe site is enlarged compared to the Mo–O_6 octahedron. This difference increases in both compounds when going to high temperature.

The magnetic structure is a simple ferromagnetic arrangement of the Fe spins. Due to the cubic structure, no information is available on the spin direction. The magnetic moment in Ba_2FeMoO_6 amounts to $\mu_{Fe} = 4.06(9)\ \mu_B$, whereas no magnetic moment was found on the Mo site within the experimental error: $\mu_{Mo} = -0.1(1)\ \mu_B$. In $BaSrFeMoO_6$ the magnetic moment values refine to $\mu_{Fe} = 4.32(8)\ \mu_B$ and $\mu_{Mo} = 0.06(10)\ \mu_B$. Taking into account the exact stoichiometry, these values yield a total effective magnetic moment of $\approx 3.63\ \mu_B$ and $\approx 4.1\ \mu_B$ for Ba_2FeMoO_6 ($Ba_2Fe_{0.92}Mo_{0.93}O_{5.7}$) and $BaSrFeMoO_6$ ($BaSrFe_{0.95}Mo_{0.97}O_{5.84}$), respectively.

Table 3. Refined structural and magnetic parameters from neutron powder-diffraction data for the Ca_2FeMoO_6 compound at 2 K (D1B), 300 K and 500 K (D2B).

	$Ca_2(Fe_{0.94(2)}Mo_{0.06(3)})Mo_{1.00(2)}O_{6.00(5)}$		
	2 K	300 K	500 K
a (Å)	5.3875(3)	5.4145(1)	5.4277(2)
b (Å)	5.5027(4)	5.5176(1)	5.5221(3)
c (Å)	7.6767(5)	7.7098(2)	7.7248(4)
β (°)	90.05(3)	90.018(8)	90.015(16)
Ca x		0.0106(5)	0.0094(12)
y		0.0436(3)	0.0429(6)
z		0.7497(11)	0.7479 (27)
O1 x		0.2901(9)	0.2907 (23)
y		0.2953(11)	0.2937 (28)
z		0.9563(8)	0.9549(15)
O2 x		0.3019(9)	0.2998(22)
y		0.2925(11)	0.2936(26)
z		0.5420(7)	0.5388(14)
O3 x		0.9203(3)	0.9217(7)
y		0.4780(3)	0.4791(6)
z		0.7519(9)	0.7521(24)
Mo–O1 (Å)		1.964(6)	1.977(14)
–O2 (Å)		1.965(6)	1.975(14)
–O3 (Å)		1.965(7)	1.965(18)
Fe–O1 (Å)		2.015(6)	2.011(15)
–O2 (Å)		2.022(5)	2.009(13)
–O3 (Å)		1.993(7)	1.997(18)
$\langle d$(Fe(Mo)–O)$\rangle$ (Å)		1.987	1.989
Mo–O1–Fe (°)		152.6(2)	152.3(6)
Mo–O2–Fe (°)		151.7(2)	152.7(6)
Mo–O3–Fe (°)		153.8(2)	154.3(4)
$\langle$Mo–O–Fe$\rangle$ (°)		152.7	153.2
μ_{Fe} (μ_B)	3.91(7)	2.53(9)	—
μ_{Mo} (μ_B)	−0.7(3)	−0.6(1)	—
R_{Bragg}	3.1	3.8	3.8
R_{Magn}	1.9	7.0	
χ^2		2.9	2.1

4.2. Ca_2FeMoO_6

High-resolution powder diffraction data were obtained at 500 K and room temperature and refined in the $P2_1/n$ space group. Structural and positional parameters are listed in table 3, which also includes the lattice parameters at 2 K (D1B). A strong tilting of the octahedron compared to the cubic structure can be realized by looking at the Fe–O–Mo angle values.

The magnetic structure is different from the first two cubic compounds since in this case a significant moment can be determined on the Mo site, oriented antiparallel to the Fe moments. While at room temperature values of $\mu_{Fe} = 2.53(9)\ \mu_B$ and $\mu_{Mo} = -0.6(1)\ \mu_B$ were found, the 2 K data reveal $\mu_{Fe} = 3.91(7)\ \mu_B$ and $\mu_{Mo} = -0.7(3)\ \mu_B$. The moments are along the b-direction. If we include a component in the c-direction, the magnetic refinement is improved but leads, however, to larger error bars. The calculated total moment amounts to $\approx$2.93 or $\approx$3.02 μ_B either considering antiparallel or parallel coupling of the 6% Mo ions on the Fe sites, respectively.

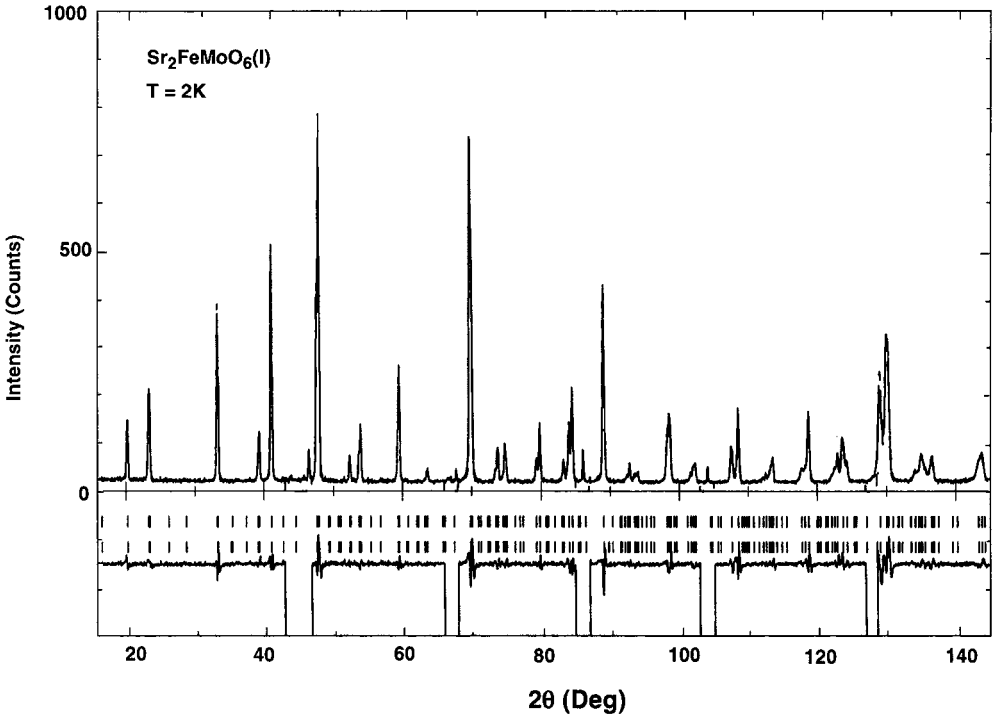

Figure 3. High-resolution neutron diffraction pattern of Sr_2FeMoO_6 (I, this work) at 2 K as recorded on D2B. Solid line is the Rietveld calculated profile. Allowed Bragg (first row of tick marks) and magnetic reflections are indicated together with the residuals (bottom).

4.3. Sr_2FeMoO_6

Two different samples were prepared and investigated, as described in the previous section with a slight difference in stoichiometry. Firstly, we will report the results on sample (I) with exact composition $Sr_2Fe_{0.97}Mo_{0.99}O_{5.96}$. When trying to refine low temperature data from D1B in order to determine the presence of any magnetic moment on the Mo site, a large discrepancy was found between the calculated and the observed peak shapes at high diffraction angles. In order to investigate further the origin of this discrepancy, a high resolution spectrum was measured at 2 K. In figures 2(a), (b) we show enlarged parts of the recorded spectra at the D2B instrument at 500 K and 2 K. Whereas the compound is cubic at 500 K, a large splitting of the peaks is clearly visible at 2 K.

An initial attempt to refine the 2 K data using the monoclinic $P2_1/n$ space group (as found for the Ca_2 compound) was not satisfactory. A tendency of the a and b cell parameters to stay equal and an angle beta of near 90 degrees indicated the existence of a tetragonal distortion. This confirms older literature data of Galasso *et al* [4] who already claimed Sr_2FeMoO_6 to be tetragonal without, however, mentioning the exact tetragonal space group and structure.

Searching for a possible tetragonal space group, we used first the pattern matching mode of the program FULLPROF [15] to restrict the possibilities. The remaining space groups were checked one by one (e.g. $P4/mmm$, $P42/nmc$ and $I4/mmm$) and finally $P4_2/m$ with reduced cell parameters $a_{tetragonal} = a_{cubic}/\sqrt{2}$ emerged as the correct space group, see figure 3. The Wyckoff positions are: Mo on 2c, Fe on 2d, Sr on 2e and 2f, O1 on 4j, O2 on 4j and O3 on 4i. When refining the 2 K data, it became quickly evident that some of the free positional

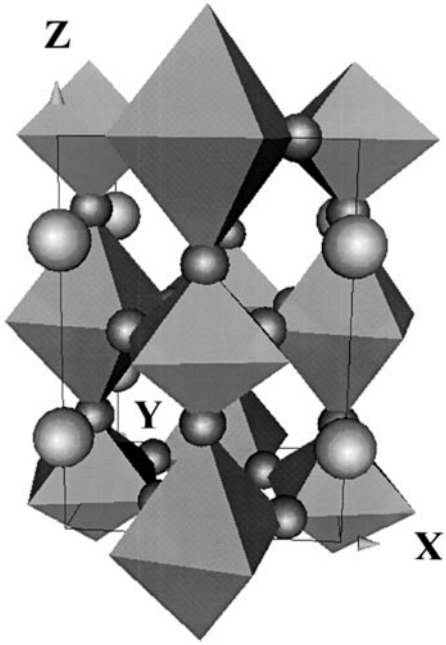

Figure 4. Schematic representation of the double perovskite structure of Sr_2FeMoO_6 in the $P4_2/m$ space group. The oxygen displacements have been exaggerated to facilitate the recognition of the principal structural features. Large/small octahedrons correspond to FeO_6/MoO_6. Small (large) spheres represent the oxygen ions (strontium).

parameters of the oxygen sublattice could be coupled as they followed a higher symmetry. A space group allowing for this higher symmetry of the oxygen sublattice is e.g. $P4_2/mbc$. Nevertheless, it cannot be used in our case for the description of the whole unit cell, as the cation sublattice is not a random distribution of Fe and Mo, but an ordered array in rock salt structure. $P4_2/mbc$ is itself a subgroup of $I4/mcm$, which in Glazer's [17] notation describes a 1 tilt system in perovskites with multiple cell $2a_p \times 2b_p \times 2c_p$. This is in fact what we find when looking closer at the $P4_2/m$ space group: figure 4 shows a schematic representation of the double perovskite structure of Sr_2FeMoO_6 in the $P4_2/m$ space group. The octahedra are solely tilted around the c-axis with the tilts being opposite at the $c = 0$ and $c = 1/2$ levels. In Glazer's notation, we are in the presence of an $a^0a^0c^-$ system. The size of the FeO_6 and MoO_6 octahedra is only different in the c-direction with Fe–O3 = 2.027(7) Å and Mo–O3 = 1.935(7) Å. The in plane cation oxygen distance amounts to Fe(Mo)–O = 1.979(1) Å, see table 4.

Using positional parameters as determined from the high resolution data, the magnetic structure of the compound was refined from the high intensity data of D1B: $\mu_{Fe} = 3.72(6)\ \mu_B$ and $\mu_{Mo} = -0.54(7)\ \mu_B$. The best fit was obtained with the spin direction parallel to the [110] direction. Magnetic moment values at 2 K as determined from the high resolution data of D2B were slightly different: $\mu_{Fe} = 3.97(10)\ \mu_B$ and $\mu_{Mo} = -0.19(11)\ \mu_B$. From these results, values of $\approx 3.07\ \mu_B$ (D1B) or $\approx 3.66\ \mu_B$ (D2B) are obtained for the total magnetic moment.

In order to determine the interplay between the structural and the magnetic transitions we decided to perform temperature dependent high-resolution diffraction measurements on D2B. Each spectrum was fitted individually; when approaching T_C, data were taken every

Table 4. Refined structural and magnetic parameters from high resolution (D2B) neutron powder-diffraction data for the Sr_2FeMoO_6 compound (I, this work) at 2 K, 200 K and 500 K. Refined magnetic parameters as determined from D1B data at 2 K has been added for comparison (*).

	$Sr_2Fe_{0.97(2)}Mo_{0.99(2)}O_{5.96(5)}$ (I)				
$P4_2/m$	2 K D2B		200 K D2B	500 K D2B	$Fm3m$
a (Å)	5.57047(9)		5.57966(6)	7.92506(10)	a (Å)
c (Å)	7.92532(16)		7.91192(15)		
O1 $x = y$	0.2741(2)		0.2708(3)	0.2519(5)	x
O2 $x = -x_{O1}$	0.2259(2)		0.2292(3)		
$y = x_{O1} + 1/2$	0.7741(2)		0.7708(3)		
O3 z	0.7558(9)		0.7527(17)		
Fe–O(1, 2) (Å)	1.979(1)		1.980(2)	1.996(4)	Fe–O (Å)
Mo–O(1, 2) (Å)	1.979(1)		1.980(2)	1.966(4)	Mo–O (Å)
Fe–O3 (Å)	2.027(7)		2.002(13)		
Mo–O3 (Å)	1.935(7)		1.959(13)		
$\langle d$(Fe(Mo)–O)$\rangle$	1.9797		1.980	1.981	
Mo–O(1, 2)–Fe (Å)	169.0(1)		170.5(1)	180	Mo–O–Fe (°)
Mo–O3–Fe (°)	180		180		
⟨Mo–O–Fe⟩	174.5		175.25	180	
μ_{Fe} (μ_B)	3.97(10)	3.72(6)*	3.04(14)	—	
μ_{Mo} (μ_B)	−0.19(11)	−0.54(7)*	−0.38(17)	—	
R_{Bragg}	3.0		3.4	4.8	
R_{Magn}	5.1		5.9	—	
χ^2	2.6		1.8	3.6	

10 K. Figure 5 displays simultaneously the temperature dependence of the tetragonal distortion defined as $1 - \sqrt{2}a/c$ and of the Fe magnetic moment. It can be immediately seen that the tetragonal distortion tends to zero as the ferromagnetic moment vanishes. In addition, one can also notice that the tetragonal distortion is increasing linearly between 390 K and 300 K. A linear increase of the Fe magnetic moment value is seen in the same temperature range. It is important to mention that since the increase of the magnetic moment seems to depend on the increase of the distortion, it does not follow a normal Brillouin-type behaviour.

Figure 6 shows the temperature dependence of the tilting angle Mo–O–Fe within the a–b-plane. It increases steadily between 169 degrees at 2 K and 177 degrees at 410 K and the approach to 180 degrees—as in a cubic system—levels off above 410 K. This reflects the fact that $P4_2/m$ is not a subgroup of $Fm3m$: the equivalence of the a–b-plane Mo–O and Fe–O distances is evidently in contradiction with the symmetry in the cubic system, where all Mo–O distances are equivalent but different from the Fe–O ones.

The detailed results available for our new Sr_2FeMoO_6 (I) sample and specially the knowledge about the existence of a structural transition from cubic to tetragonal taking place in this sample below T_C gave us reasons to partly reinvestigate our previous Sr_2FeMoO_6 (II) sample, already published in [9]. The new data set measured at 500 K on D2B allowed us to determine the exact stoichiometry to be $Sr_2Fe_{0.97}Mo_{0.94}O_{5.81}$ as we have already commented. Using this information, we refined the room temperature data set in the space group $P4_2/m$. The fit converged nicely and gave structural and positional parameters shown in table 5. The tetragonal distortion is slightly lower than in the other Sr_2FeMoO_6 (I) compound, explaining why we did not notice the tetragonal symmetry in the first instance [9]. The magnetic refinement yields at room temperature $\mu_{Fe} = 2.7(4)\ \mu_B$ and $\mu_{Mo} = 0.03(51)\ \mu_B$, values identical to the other Sr_2FeMoO_6 (I) sample (see figure 6). The 2 K data set measured at the high intensity

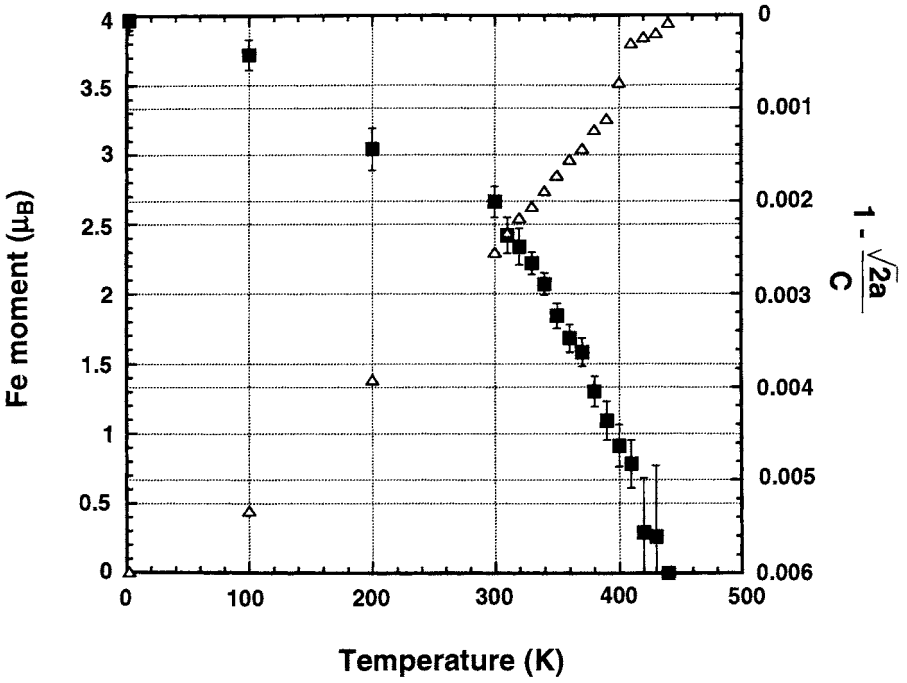

Figure 5. Thermal dependence of Fe magnetic moment (■) and tetragonal distortion $1 - \sqrt{2}a/c$ (△) for the Sr_2FeMoO_6 compound as determined from the Rietveld analysis of the high resolution neutron diffraction spectra.

machine D20 was now refined as well in $P4_2/m$ and gave better results compared to the originally supposed $Fm3m$ space group. A small magnetic moment was now found as well on the Mo site: $\mu_{Fe} = 3.95(6)\ \mu_B$ and $\mu_{Mo} = -0.42(6)\ \mu_B$, giving an effective total moment of $\approx 3.44\ \mu_B$.

5. Discussion

Reasonable agreement has been found between the total effective magnetic moments as determined from the neutron diffraction Rietveld analysis (see tables 2–5) and the saturation magnetic moments determined from magnetization measurements (see table 1), as already commented in the previous section. This confirms the proposed ferrimagnetic ordering between Fe and Mo magnetic moments. We must emphasize that the comparison should be made taking into account the exact stoichiometry of the compounds, and, therefore, a detailed high temperature high resolution study is indispensable before attempting any reliable refinement of the magnetic structure. From our neutron diffraction results, no evidence of mis-site cation disorder has been found (except for a small 6% of Mo on the Fe sites in the Ca_2FeMoO_6 sample), also in agreement with our x-ray diffraction study at room temperature (section 3). Therefore, the smaller values obtained when compared to the ideal 4 μ_B fu^{-1} value must be ascribed to off-stoichiometry, i.e. Fe, Mo and O vacancies. In particular, the role of the oxygen vacancies has been suggested to strongly influence both saturation magnetization and Curie temperature [7].

In order to find a more in-depth correlation between the crystallographic and magnetic

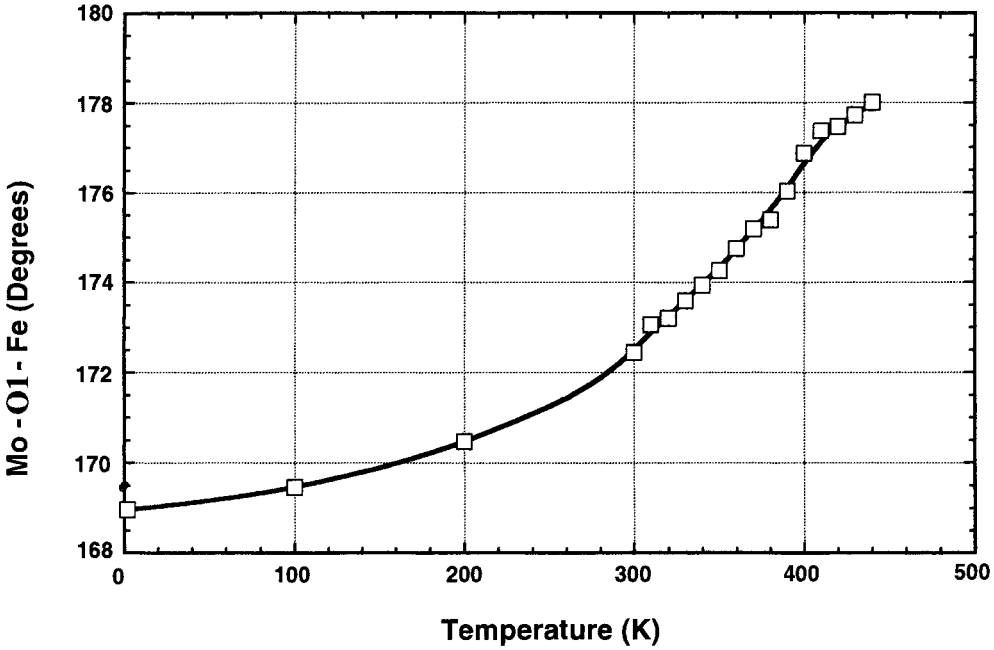

Figure 6. Thermal dependence of the Mo–O1–Fe bond angle for the Sr_2FeMoO_6 compound as determined from the Rietveld analysis of the high resolution neutron diffraction spectra. The line is a guide to the eye.

properties of this series of double perovskites $AA'FeMoO_6$ ($AA' = Ba_2$, BaSr, Sr_2, Ca_2), the evolution of the Curie temperature and crystallographic structure as a function of the average ionic radius $\langle r_A \rangle$ are displayed in figure 7. As $\langle r_A \rangle$ is increased, the symmetry of the crystallographic structure increases from monoclinic (Ca_2) to tetragonal (Sr_2) and finally to cubic (BaSr and Ba_2). This can be ascribed to steric effects, as widely observed in the manganites [18], and has a profound impact on structural parameters important for the electronic structure. In this sense, we observe that the maximum T_C is achieved for the Sr_2FeMoO_6 compound. Although it may be argued that the exact T_C values are sample dependent, this trend appears to be always verified (see e.g. [4]). An important parameter that might be responsible for the observed behaviour is the bare electronic bandwidth W, which is controlled by structural parameters, as has been reported in the case of $A_{1-x}A'_xMnO_3$ [18]. For perovskite compounds ABX_3, it is straightforward in a tight-binding approximation that W should depend on both B–X bond lengths and B–X–B bond angles through the overlap integrals of 3d(B)–2p(X) orbitals. The following empirical formula has been successfully used [18, 19]:

$$W \approx \frac{\cos\omega}{d_{B-X}^{3.5}} \tag{1}$$

where ω is the 'tilt' angle in the plane of the bond, given by $\omega = (\pi - \langle \text{B–X–B} \rangle)/2$, and d_{B-X} is the B–X bond length. Both are structural parameters that can be determined in our compounds from the data in tables 2–5. We have taken averaged values over the crystallographically independent O positions and for both Fe and Mo ions at $T = 500$ K. No significant difference is found if one uses structural data at room temperature in the compounds where available. The values of W thus estimated are also shown in figure 7 as a function of $\langle r_A \rangle$ for comparison. We

Table 5. Refined structural and magnetic parameters from neutron powder-diffraction data for the Sr_2FeMoO_6 compound (II, sample used in a previous publication [9]) at 2 K (D20), 300 K and 500 K (D2B).

	$Sr_2Fe_{0.97(2)}Mo_{0.94(2)}O_{5.81(5)}$ (II)			
$P4_2/m$	2K D20	300 K D2B	500 K D2B	$Fm3m$
a (Å)	5.5741(3)	5.5873(6)	7.919 04(9)	a (Å)
c (Å)	7.9243(6)	7.9180(12)		
O1 $x = y$	0.2727(3)	0.2657(13)	0.2530(5)	x
O2 $x = -x_{O1}$	0.2273(3)	0.2343(13)		
$y = x_{O1} + 1/2$	0.7727(3)	0.7657(13)		
O3 z	0.7544(17)	0.7500 fixed		
Fe–O(1, 2) (Å)	1.979(2)	1.979(7)	2.003(4)	Fe–O
Mo–O(1, 2) (Å)	1.979(1)	1.979(7)	1.956(4)	Mo–O
Fe–O3 (Å)	2.016(14)	1.980		
Mo–O3 (Å)	1.946(14)	1.980		
$\langle d$(Fe(Mo)–O)$\rangle$	1.9797	1.9793	1.9795	
Mo–O(1, 2)–Fe (°)	169.6(1)	172.8(4)	180	Mo–O–Fe (°)
Mo–O3–Fe (°)	180	180		
⟨Mo–O–Fe⟩	174.8	176.4	180	
μ_{Fe} (μ_B)	3.95(6)	2.7(4)	—	
μ_{Mo} (μ_B)	−0.42(6)	0.03(51)	—	
R_{Bragg}	1.9	4.3	5.9	
R_{Magn}	1.8	7.5	—	
χ^2		2.2	2.9	

can observe a remarkable correlation between the dependence of both T_C and W as a function of $\langle r_A \rangle$. This strongly indicates that the observed variation in T_C can be explained by changes in the W parameter, i.e. the maximum T_C value for Sr_2FeMoO_6 corresponds to the compound with a larger estimated electronic bandwidth W.

Band calculations indicate the presence of Fe, Mo and O spin-down sub-bands crossing the Fermi level [3], which can provide the conduction mechanism through a kind of double-exchange interaction Fe–O–Mo. This picture is supported by our neutron results, which show that, when different from zero, the Mo magnetic moment is antiparallel to the Fe magnetization. Moreover, the observed correlation between the Curie temperature and the electronic bandwidth seems to indicate that the double exchange mechanism would be in a first approximation controlled by structural parameters. Should this analysis be correct, one would expect that for a given number of electrons in the conduction band, a higher Curie temperature would be coupled to a higher conductance. Resistivity measurements in single crystals could shed light on this issue.

6. Summary

In summary, we have presented a detailed crystallographic and magnetic characterization of the double perovskites $AA'FeMoO_6$ ($AA' = Ba_2$, BaSr, Sr_2, Ca_2) by means of room-temperature x-ray diffraction, magnetization measurements and neutron diffraction. Our results are consistent with a ferrimagnetic coupling of the Fe and Mo magnetic moments in all the compounds. No evidence of significant mis-site cation disorder has been found either by x-ray or neutron diffraction. Therefore, the smaller values obtained when compared to the ideal 4 μ_B fu^{-1} value must be ascribed to off-stoichiometry effects, i.e. Fe, Mo and O

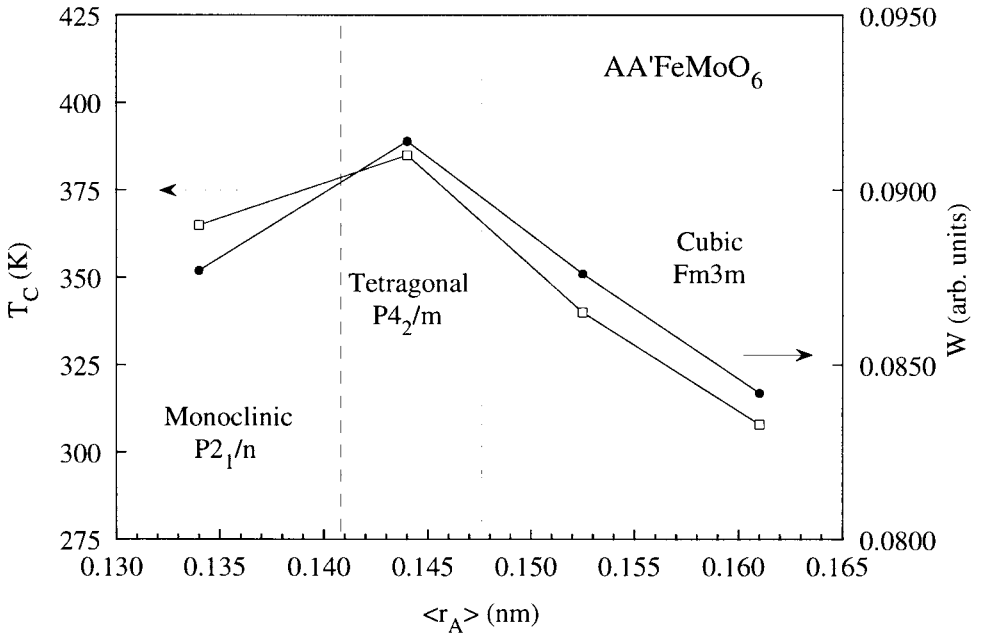

Figure 7. Comparison of the evolution of the electronic bandwidth W (●) (see text) and of the Curie temperature T_C (□) as a function of the average ionic radius $\langle r_A \rangle$.

vacancies. As the average ionic radius decreases, the crystallographic structure evolves from cubic ($AA' = Ba_2$, BaSr) to tetragonal (Sr_2) and finally to monoclinic (Ca_2). In the case of Sr_2FeMoO_6, a crossover from a high temperature paramagnetic cubic ($Fm3m$) state to a low temperature ferrimagnetic tetragonal ($P4_2/m$) state has been observed. We have also suggested the existence of a remarkable correlation between the Curie temperature and the electronic bandwidth W, in particular responsible for the evolution of T_C as a function of the average ionic radius $\langle r_A \rangle$.

Acknowledgments

The Spanish authors are grateful to the Spanish CICYT for financial support under grant Nos MAT99-0847 and MAT99-1063-C04-01. The EC project GRD1-1999-10502 (AMORE) is also acknowledged.

References

[1] Prinz G 1998 *Science* **282** 1660
[2] Gupta A and Sun J Z 1999 *J. Magn. Magn. Mater.* **200** 24
[3] Kobayashi K I, Kimura T, Sawada H, Terakura K and Tokura Y 1998 *Nature* **395** 677
[4] Galasso F S, Douglas F C and Kasper R J 1966 *J. Chem. Phys.* **44** 1672
[5] Nakagawa T J 1968 *Phys. Soc. Japan* **24** 806
[6] Borges R P, Thomas R M, Cullinan C, Coey J M D, Suryanarayanan R, Ben-Dor L, Pinsard-Gaudart L and Revcolevschi A 1999 *J. Phys.: Condens. Matter* **11** L445
[7] Ogale A S, Ogale S B, Ramesh R and Venkatesan T 1999 *Appl. Phys. Lett.* **75** 537
[8] Sleight A W and Weiher J F 1972 *J. Phys. Chem. Solids* **33** 679

[9] García-Landa B, Ritter C, Ibarra M R, Blasco J, Algarabel P A, Mahendiran R and García J 1999 *Solid State Commun.* **110** 435
[10] Maignan A, Raveau B, Martin C and Hervieu M 1999 *J. Solid State Chem.* **144** 224
[11] Kim T H, Uehara M, Cheong S-W and Lee S 1999 *Appl. Phys. Lett.* **74** 1737
[12] Asano H *et al* 1999 *Appl. Phys. Lett.* **74** 3696
[13] Manako T, Izumi M, Konishi Y, Kobayashi K I, Kawasaki M and Tokura Y 1999 *Appl. Phys. Lett.* **74** 2215
[14] Yin H Q, Zhou J-S, Zhou J-P, Dass R, McDevitt J T and Goodenough J B 1999 *Appl. Phys. Lett.* **75** 2812
[15] Rodríguez-Carvajal J 1993 *Physica* B **192** 55
[16] Tomioka Y, Okuda T, Okimoto Y, Kumai R, Kobayashi K I and Tokura Y 2000 *Phys. Rev.* B **61** 422
[17] Glazer A M 1975 *Acta Crystallogr.* A **31** 756
[18] Radaelli P G, Iannone G, Marezio M, Hwang H Y, Cheong S-W, Jorgensen J D and Argyriou D N 1997 *Phys. Rev.* B **56** 8265
[19] Medarde M, Mesot J, Lacorre P, Rosenkranz S, Fischer P and Gobrecht K 1995 *Phys. Rev.* B **52** 9248